Proceedings of
The 5th National Congress on Fluids Engineering
March 26-28. 2008, Jeju, Korea

Hysteric Transient Phenomenon of Under-Expanded Moist Air Jets

S. J. Oh*, C. S. Shin*, H. D. Kim* and T. Setoguchi**

부족팽창 습공기 제트의 히스테리과도현상

오성진* · 신춘식* · 김희동* · T. Setoguchi**

Key Words : *Compressible flow(압축성 유동), Supersonic jet(초음속 제트), Shock wave(충격파), Nonequilibrium condensation(비평형 응축)*

Abstract

the present study, the addresses the hysteric phenomenon of under-expanded jets with a help of a computational fluid dynamics methods. The under-expanded jets of both dry and moist air have been employed to the transient processes for the pressure ratio. It is known that under-expanded air jet produced during the process of increase in pressure ratio behaves different from the reducing process, leading to a hysteric phenomenon of under-expanded jet. It is also known that moist air jet significantly reduces the hysteric phenomenon found in the dry air jet, and that non-equilibrium condensation which occurs in the under-expanded moist air jet is responsible for these findings.

1. Introduction

In generally, the pressure ratio and nozzle geometry are given, the structures of under-expanded jet are well known. As the pressure ratio increases over a critical value, corresponding to a sonic condition at the exit of nozzle, regular reflection of shock wave occurs in the weakly under-expanded jet. Then, as the pressure increases further, the regular reflection transitions to Mach reflection, leading to the Mach disk on the jet axis. On the contrary, the Mach reflection reduces again to the regular reflection, as the jet pressure ratio decreases.

Recently, Otobe et al. have observed that a hysteresis phenomenon of the under expanded jet is produced during the change of pressure ratio, in which the jet flow obtained in the increase process of the pressure ratio is different from that in the process of decreasing pressure ratio. In many industrial and engineering applications of under-expanded jets, the jet pressure ratio is changing during the process. However, only a few works have, to date, devoted to the jet hysteresis, but its physical reasoning is still not satisfactorily known. Moreover, there is no work to investigate the hysteresis phenomenon in under-expanded moist air jets, so far.

In the present study, the under-expanded moist air jets, corresponding to the range of moderately expanded to strongly expanded conditions have been investigated with a help of a computational fluid dynamics method. The jet pressure ratio is changed to obtain the hysteresis phenomena. Quasi steady computational analysis is carried out to numerically solve the axisymmetric, compressible Euler equations. Initial relative humidity at the nozzle supply is varied to get different moist air jets. The present computations are validated with the experimental data. The results obtained show that the hysteresis behavior appears in both dry and moist air jets, but the moist air jets leads to much less hysteresis, compared with the dry air jets.

* Andong National University, kimhd@andong.ac.kr
** Saga University, Japan,

2. research Method

2.1 Computational Conditions

Moist air as a working gas is issued from the nozzle exit. The pressure ratio, which is defined as the ratio of the reservoir pressure p0(atmospheric pressure) to the back pressure pb, is denoted by ϕ. In the present study, ϕ varies from 3.0 to 6.2. Furthermore, the initial degree of supersaturation S0 is adjusted such that it is between 0 and 0.8. The reservoir total temperature T0 and total pressure p0are 298.15K and 101.3kPa, respectively.

A fixed boundary condition was applied to the upstream boundary of the computational domain and the downstream boundaries were taken as outflow condition. Along the nozzle wall surfaces, adiabatic and non-slip

boundary conditions were assumed.

Figure 1 shows the computational grids of the flow field. The sonic nozzle is a cylindrical straight nozzle having a diameter of De=12.7mm (characteristic length) at the exit and a radius of curvature R=De at the entrance. The straight section, which has a length of 0.4De, is followed by the convergent section. The nozzle shape is the same as that used by Addy[4]. The upper side shows the grid number and the lower side shows the boundary conditions.

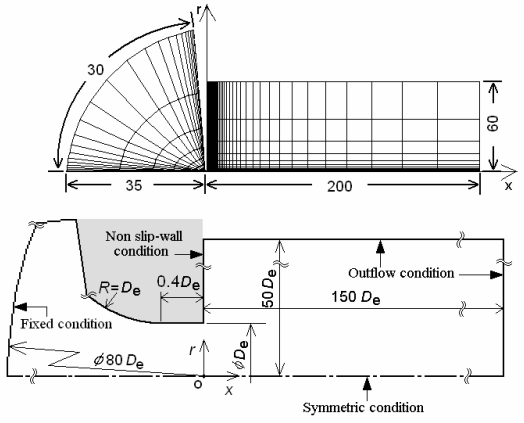

Figure 1. Computational grid, domain and boundary conditions.

2.2 Comparison with experimental results

Experiments were conducted in order to verify of calculated results. The reservoir pressure and back pressure are the same as computational ones. The range of the pressure ratio ϕ is from 3.6 to 6.4. Values of the initial degree of supersaturation S0 are 0.15 (this seems to be dry air), 0.4 and 0.7.The flow field was investigated by a schlieren optical method.

Figure 2 and Fig.3 show comparisons of contour maps of density obtained by calculation in a steady state with schlieren photographs for ϕ=3.8 and 6.2, respectively. For the applied pressure ratios, the jet is under-expanded at the nozzle exit. Results for dry air and S0=0.7 are also shown in each figure. As seen from these figures, the flow structures obtained by simulation are similar to experimental results and the validity of the present simulation is confirmed by comparison with the experiments.

In Fig.2(a), an oblique shock wave is observed in the flow field. In case of non-equilibrium condensation (Fig.2(b)), density gradient in Prandtl-Meyer expansion fan is slightly changed in comparison with the case of dry air

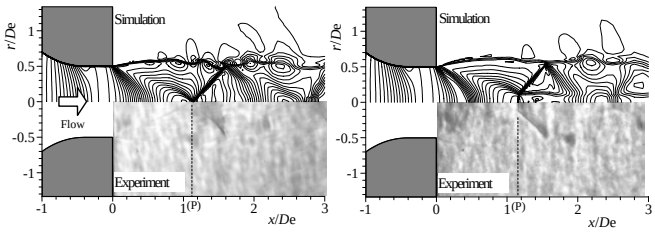

(a) S_0=0 (b) S_0=0.7

Figure 2. Comparisons between simulated and experimental results(ϕ=3.8)

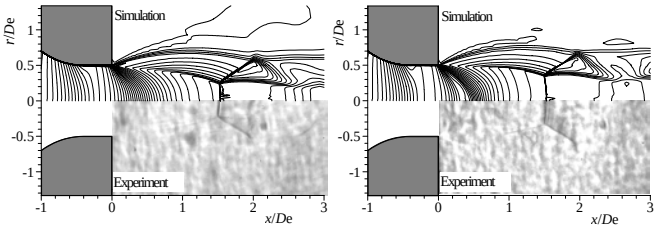

(a) S_0=0 (b) S_0=0.7

Figure 3. Comparisons between simulated and experimental results(ϕ=6.2)

(Fig.2(a)) due to the latent heat released by the homogeneous condensation. Furthermore, Mach disk appears at the position x/D_e=1.16. However, there is little change in the distance P from the nozzle exit for cases of dry air and S_0 =0.7.

In Fig.3(b), density gradients in Prandtl-Meyer expansion fan is slightly changed in comparison with the case of no condensation (Fig.3(a)) due to the latent heat released by the non-equilibrium condensation. Furthermore, there is also not much change in the position of Mach disk as the case of ϕ=3.8 (Fig.2). However, the diameter of the Mach disk becomes lager with an increase of S_0.

2.3 Transition of reflection type

Figure 4 shows three types of jet structure for dry air (S_0=0). The upper figures show the pressure contour map

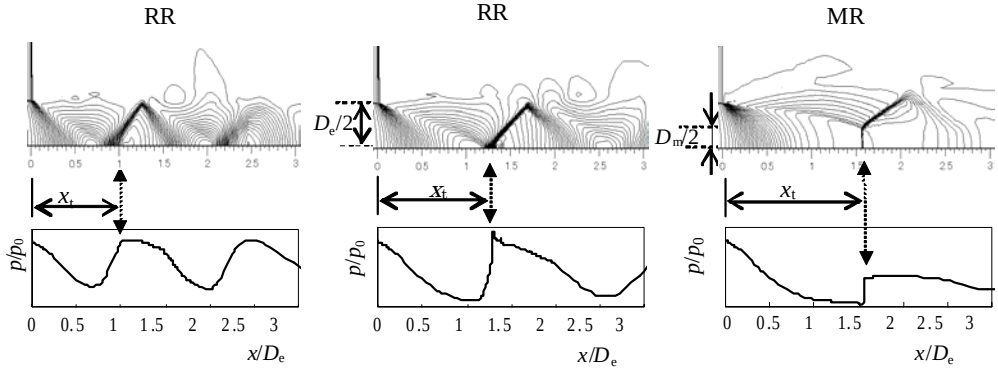

(a) ϕ=3.0 (b) ϕ=4.0 (c) ϕ=6.0

Figure 4. Three patterns of under-expanded dry air jet (S_0=0).

and the lower figures show the pressure distribution along the jet axis. In Fig. 4(a), the structure is cell mode and the pressure wave is similar to a sine wave. In Fig. 4(b), the barrel shock waves formed in the jet intersect with each other at the jet axis and the pressure along the jet axis has a maximum value at the intersection point (defined by the symbol x_t.). The reflection type is a Regular Reflection (RR). In Fig. 4(c), a Mach disk occurs in the jet and the pressure makes a sudden upturn at the position of the Mach disk (defined by symbol x_t.). The reflection type is a Mach Reflection (MR).

2.4 Pressure distribution along jet axis

Figure 5 shows the pressure distributions along the jet axis for supersonic flow with the same conditions as those shown in Fig. 3. The black lines (shown in the figure) represent the results obtained using the Down process and the gray lines represent the results obtained using the Up process. For dry air (Fig.5(a)), the difference between Up and Down, for ϕ=4.5, is large. For moist air (Fig. 5(b)) the difference between Down and Up for ϕ=4.3 is noticeable, however, it is not as large as for dry air. In the case of moist air, the pressure increases occur between the nozzle exit and the Mach disk. This pressure increases seems to be due to the latent heat released by the condensation.

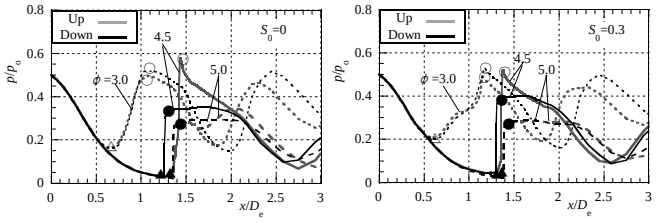

(a) S_0=0 (b) S_0=0.3

Figure 5. Static pressure distribution on jet axis.

Figure 6 shows the nondimensional overpressure $\Delta p/p_0$ which represents the difference between the pressure distributions for S_0=0.3 and S_0=0, for the Up process. The black lines in the plots represent the overpressure for MR and the gray lines represent the overpressure for RR. The overpressures begin at about x/D_e=0.4 for all pressure ratios. The peaks of overpressure and the peak positions for RR vary differ widely, however the curves for MR are almost the same.

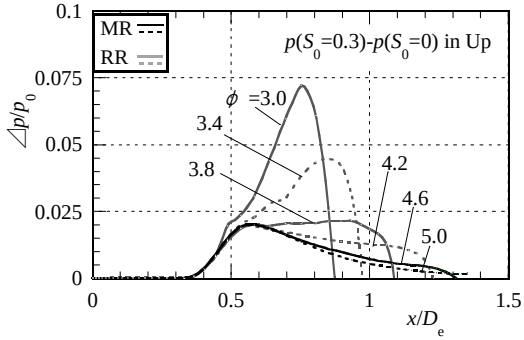

Figure 6. Difference between the static pressure distributions of dry and moist air jets.

Figure 7 shows the progress of pressures on the upper and lower surfaces of the Mach disk, for dryAN air. Figure 7(a) shows the pressure progress for the process of increasing pressure ratio and Fig. 7(b) shows the pressure progress for the process of decreasing pressure ratio. Pressures for a steady jet about the transition pressure ratio are also presented for comparison purposes. The pressures just upstream and downstream of shock wave are represented by the same markers as those used in Fig. 5(a).

The pressures just upstream of shock wave are almost the same for the Up, Down and steady. On the other hand, the differences between the Up and Down and between the steady and quasi-steady pressures just downstream of shock wave(about the transition pressureratio), are remarkable. In the figures, the shadow areas show the range of the pressure ratio for MR.

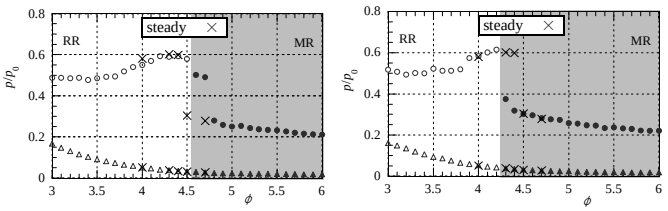

(a) the process of increasing pressure ratio (S_0=0) (b) the process of decreasing pressure ratio (S_0=0)

Figure 7. Variation in the static pressures just upstream and downstream of shock wave.

2.5 Hysteresis for x_t/D_e

Figure 8(a) and 8(b) show the relationships between pressure ratio ϕ and position x_t, for dry air (S_0=0) and moist air (S_0=0.3) respectively. The marker circles in the figures represent the Down process and the marker triangles represent the Up process. An open maker represents a RR and a closed maker represents a MR.

For the Down process, the non-dimensional position x_t/D_e initially decreases with pressure ratio ϕ. It increases once just before the transition of reflection type at ϕ=4.3 for Fig. 8(a) and at ϕ=4.2 for Fig. 8(b). It decreases thereafter. On the other hand, for Up process, the position x_t/D_e increases with pressure ratio ϕ. However it decreases once just after the transition of reflection type (at ϕ=4.8 for Fig. 8(a) and at ϕ=4.5 for Fig. 8(b)).It increases thereafter.

The graph traces other routes, for the Up and Down processes, in the region where the reflection type changes, but it follows the same course in other regions. Therefore it can be concluded that hysteresis phenomena have occurred between x_t and ϕ.

The hysteresis loop shown in Fig. 8(b) is smaller than the one shown in Fig. 8(a) because the routes in Up process are different though there are not so many differences in Down.

Figure 8. Variation in the Mach disk distance with the process of change of pressure ratio in both dry and moist air jets.

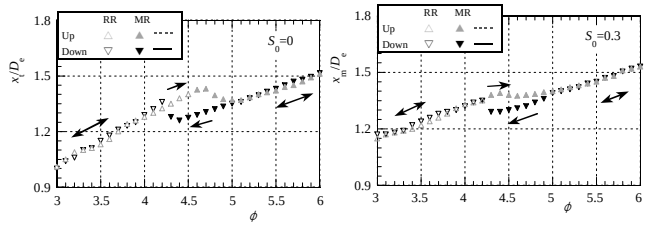

(a) S_0=0 (b) S_0=0.3

2.6 Hysteresis for D_m/D_e

Figure 9(a) and 9(b) show the relationships between pressure ratio ϕ and non-dimensional Mack disk diameter D_m/D_e, for dry air (S_0=0) and for moist air (S_0=0.3) respectively. The makers used are the same as those used in Fig. 5. The non-dimensional diameter D_m/D_e decreases or increases with the pressure ratio ϕ, for a Mach Reflection (MR). However D_m/D_e is 0 for a Regular Reflection (RR). The transitional pressure ratio ϕ^u_{tr} in the Up process is bigger than the transitional pressure ratio ϕ^d_{tr} for the Down process, in both Fig. 9(a) and 9(b).

Therefore it can be concluded that hysteresis phenomena between D_m/D_e and ϕ have occurred. Comparing Fig. 9(a) and 9(b), the hysteresis loop shown in Fig. 9(b) is smaller than the one shown in Fig. 9(a) because the difference between ϕ^u_{tr} and ϕ^d_{tr} is smaller for moist air than for dry air.

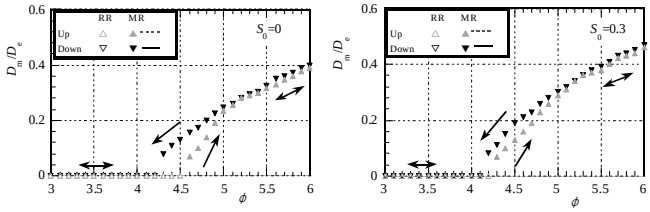

(a) S_0=0 (b) S_0=0.3

Figure 9. Variation in the Mach disk diameter with the process of change of pressure ratio in both dry and moist air jets.

3. Results and Discussion

Numerical computations were performed to investigate the hysteresis phenomenon of a Mach disk in an under-expanded sonic jet with condensation. The results are as follows.

(1) The transitional pressure ratio of a reflection type in Down process ϕ^d_{tr} is smaller than the transitional pressure ratio of reflection type in Up process ϕ^u_{tr} in an under-expanded sonic jet. In the case of moist air with condensation, the transitional pressure ratio of reflection type ϕ_{tr} becomes small.

(2) The hysteresis phenomenon occurs between the position x_t (the intersection point in RR or the location of Mach disk in MR) and pressure ratio ϕ. In the case of moist air with condensation, the hysteresis loop becomes small compared to dry air.

(3) The hysteresis phenomenon occurs between the Mach disk diameter D_m and pressure ratio ϕ. In the case of moist air with condensation, the hysteresis loop becomes small compared to dry air.

References

[1] *Man H.C.*:, Dynamics Characteristics of Gas Jets from Subsonic and Supersonic Nozzles for High Pressure Gas Laser Cutting, Optics & Laser Technology, No. 30, (1998), pp. 497

[2] *Kim, H. D. Lee, J. S.*: An Experimental Study on Supersonic Jet Issuing from Gas Atomizing Nozzle (part 1), Journal of Korea Society of Mechanical Engineers, Ser.(B), Vol. 20, No. 2, (1996), pp. 677-709

[3] *Chang, I. S. Chow, W. L.*: Mach Disk from Under-expanded Axisymetric Nozzle Flow, AIAA Journal, Vol. 12, No.8, (1974), pp. 1079-1082

[4] *Addy, A. L.*: Effects of Axisymetric Sonic Nozzle Geometry on Mach Disk Characteristics, AIAA Journal, Vol. 19, No. 1, (1981), pp. 121-122

[5] *Gribben, B. J. Badcock, K. J. Richards, B. E.*: Numerical Study of Shock-Reflection Hysteresis in an Underexpanded Jet, AIAA Journal, Vol. 38, No. 2, (2000), pp. 275-283

[6] *Deck, S.*: Unsteady Side Loads in a Thrust-Optimized Contour Nozzle at Hysteresis Regime, AIAA Journal, Vol. 42, No. 9, (2004), pp. 1878-1888

[7] *Irie, T.; Yasunobu, T.; Kashimura, H.; Setoguchi, T.*: Hysteresis Phenomena of Mach Disk Formation in an Underexpanded Jet, Theoretical and Applied Mechanics Japan, Vol. 53, (2004), pp. 181-187

[8] *Sislian, J. P.*: Condensstion of water vapour with or without a carrier gas in a shock tube, UTIAS Report, (1975), pp. 201

[9] *Adam, S.*: Numerische und Experimentelle Untersuchung Instationarer Dusenstromungen mit Energiezufuhr durch Homogene Kondensation, Dissertation, Fukaltat fur Maschinenbau, Universitat Karlsruhe (TH), Germany (1999)

[10] *Matsuo, S., Otobe, Y., Tanaka, M., Kashimura, H.; Setoguchi, T. Yu, S.*: Effect of Non-equilibrium Condensation on Axisymmetric Under-expanded Jet, International Journal of Turbo and Jet Engines, Vol. 21, (2004), pp. 193-201

[11] C *Yee, H. C.*: A Class of High-Resolution Explicit and Implicit Shock Capturing Methods, NASA TM-101088, (1989)